Rescue of tomato spotted wilt virus entirely from complementary DNA clones

Mingfeng Feng[a], Ruixiang Cheng[a], Minglong Chen[a], Rong Guo[a], Luyao Li[a], Zhike Feng[a], Jianyan Wu[a], Li Xie[b], Jian Hong[b], Zhongkai Zhang[c], Richard Kormelink[d], and Xiaorong Tao[a,1]

[a]Department of Plant Pathology, Nanjing Agricultural University, 210095 Nanjing, People's Republic of China; [b]Analysis Center of Agrobiology and Environmental Sciences, Zhejiang University, 317502 Hangzhou, People's Republic of China; [c]Yunnan Provincial Key Laboratory of Agri-Biotechnology, Institute of Biotechnology and Genetic Resources, Yunnan Academy of Agricultural Sciences, 650223 Kunming, People's Republic of China; and [d]Laboratory of Virology, Department of Plant Sciences, Wageningen University, 6708PB Wageningen, The Netherlands

Edited by David C. Baulcombe, University of Cambridge, Cambridge, United Kingdom, and approved December 2, 2019 (received for review June 26, 2019)

Negative-stranded/ambisense RNA viruses (NSVs) include not only dangerous pathogens of medical importance but also serious plant pathogens of agronomic importance. Tomato spotted wilt virus (TSWV) is one of the most important plant NSVs, infecting more than 1,000 plant species, and poses major threats to global food security. The segmented negative-stranded/ambisense RNA genomes of TSWV, however, have been a major obstacle to molecular genetic manipulation. In this study, we report the complete recovery of infectious TSWV entirely from complementary DNA (cDNA) clones. First, a replication- and transcription-competent minigenome replication system was established based on 35S-driven constructs of the $S_{(-)}$-genomic (g) or $S_{(+)}$-antigenomic (ag) RNA template, flanked by the 5′ hammerhead and 3′ ribozyme sequence of hepatitis delta virus, a nucleocapsid (N) protein gene and codon-optimized viral RNA-dependent RNA polymerase (RdRp) gene. Next, a movement-competent minigenome replication system was developed based on $M_{(-)}$-gRNA, which was able to complement cell-to-cell and systemic movement of reconstituted ribonucleoprotein complexes (RNPs) of S RNA replicon. Finally, infectious TSWV and derivatives carrying eGFP reporters were rescued *in planta* via simultaneous expression of full-length cDNA constructs coding for $S_{(+)}$-agRNA, $M_{(-)}$-gRNA, and $L_{(+)}$-agRNA in which the glycoprotein gene sequence of $M_{(-)}$-gRNA was optimized. Viral rescue occurred with the addition of various RNAi suppressors including P19, HcPro, and γb, but TSWV NSs interfered with the rescue of genomic RNA. This reverse genetics system for TSWV now allows detailed molecular genetic analysis of all aspects of viral infection cycle and pathogenicity.

reverse genetics system | tomato spotted wilt virus | negative-strand RNA virus | minireplicon | genome-length infectious cDNA clones

Negative-stranded/ambisense RNA viruses (NSVs) include well-known members of medical importance such as Ebola virus (EBOV), rabies virus (RV), influenza A virus (FLUAV), and Rift Valley fever virus (RVFV) (1, 2), which can cause considerable morbidity and mortality in humans and burden national health care budgets. NSVs also include serious plant pathogens of agricultural importance, such as Tospoviruses, Tenuiviruses, and Rhabdoviruses, that cause severe diseases on agronomic crops and pose major threats to global food security (3–13).

NSVs can be classified into nonsegmented and segmented viruses. Nonsegmented NSVs (*Mononegavirales*) contain single genomic RNA segments, whereas Arenaviruses, Bunyaviruses, and Orthomyxoviruses contain 2, 3, and 6 to 8 segmented RNAs, respectively. Tospoviruses have 3 segments (tripartite) and rank among the most devastating plant viruses worldwide (14, 15). They are classified in the family *Tospoviridae* within the order *Bunyavidales* (16). *Tomato spotted wilt virus* (TSWV) is the type member of the only genus *Orthotospovirus* in the family *Tospoviridae* (14, 16). TSWV has very broad host range, infecting more than 1,000 plant species over 80 families (17), and is transmitted by thrips in a persistent, propagative manner (6, 9, 18, 19). Crop losses due to this virus have been estimated at more than $1 billion annually (7, 17).

TSWV consists of spherical, enveloped virus particles (80 to 120 nm) that contain a tripartite genome consisting of large- (L), medium- (M), and small-sized (S) RNA segments (14). The L RNA segment is negative sense and encodes a single large RNA-dependent RNA polymerase (RdRp, ~330 kDa) that is required for viral RNA replication and mRNA transcription (20, 21). Both M and S RNA segments are encoded as ambisense. The genomic (g) RNA (designated [−]) of the M segment encodes a nonstructural protein (NSm), and the antigenomic (ag) RNA (designated [+]) of the M segment encodes a precursor to the glycoproteins (GP; Gn and Gc, with n and c referring to the amino- and carboxyl-terminal ends of the precursor, respectively). The NSm plays pivotal roles in cell-to-cell and long-distance movement of TSWV (22–26). The glycoproteins are required for particle maturation and are present as spikes on the surface of the virus envelope membrane (27, 28). They also play a major role as determinants for thrips vector transmission (29). The gRNA of the S segment encodes a nonstructural protein (NSs), and the agRNA of the S segment codes for a nucleocapsid protein (N). The NSs protein functions as an RNA silencing suppressor to defend against the plant innate immunity system (30–32) and triggers a defense response and concomitant programmed cell death mediated by the dominant resistance gene

Significance

Although reverse genetics (RG) systems were first developed for animal-infecting viruses with segmented negative-stranded/ambisense RNA genomes over 20 years ago, such a system for plant viruses with segmented negative-stranded/ambisense RNA genomes had not been developed until now. Tomato spotted wilt virus (TSWV), a virus with tripartite negative-stranded/ambisense RNA genomes, is one of the most economically important plant viruses in the world. Many groups have tried to construct infectious clones for TSWV, but all have failed. Here we report the establishment of a RG system for TSWV. Infectious TSWV and derivatives carrying eGFP reporters were rescued entirely from complementary DNA (cDNA) clones. This RG system now provides a powerful platform to study the disease pathology of Tospoviruses during natural infection.

Author contributions: M.F., Z.F., and X.T. designed research; M.F., R.C., M.C., R.G., L.L., Z.F., J.W., L.X., J.H., and Z.Z. performed research; M.F. contributed new reagents/analytic tools; M.F. analyzed data; and M.F., R.K., and X.T. wrote the paper.

The authors declare no competing interest.

This article is a PNAS Direct Submission.

[1]To whom correspondence may be addressed. Email: taoxiaorong@njau.edu.cn.

This article contains supporting information online at https://www.pnas.org/lookup/suppl/doi:10.1073/pnas.1910787117/-/DCSupplemental.

First published December 26, 2019.

Tsw from *Capsicum chinense* (33–35). The N protein participates in the formation of ribonucleoprotein complexes (RNPs) (36–38) and is required for viral intracellular movement (39, 40).

As a virus intensively studied for almost a century (7, 41), TSWV has served as an important model for studying the molecular biology of *Tospovirus* and other plant NSVs with segmented genomes (6–8, 14). However, its negative-stranded/ambisense tripartite RNA genomes have posed a major obstacle to genetic manipulation of the virus. The initiation of an infection cycle with this virus requires at least the RNP, the minimal infectious unit that consists of viral RNA encapsidated by the N protein and associated with a few copies of the viral RNA-dependent RNA polymerase (6, 14). TSWV RNPs can be mechanically transferred from infected to healthy plants; however, transmission by thrips requires RNPs to be enveloped and spiked with the glycoproteins (29).

The first animal-infecting and related counterpart of TSWV with a segmented RNA genome to be rescued entirely from complementary DNA (cDNA) was Bunyamwera virus in 1996 (42). Following this study, soon other segmented NSVs were rescued from plasmid DNA. The influenza A virus, containing a genome of 8 RNA segments, was recovered in 1999 (43), while the first arenavirus, with a bipartite RNA genome, was recovered in 2006 (44). The rescue of the first nonsegmented plant NSV from the *Mononegavirales*, i.e., the sonchus yellow net virus (SYNV), was not reported until recently (11, 45). More recently, a TSWV S RNA-based minireplicon in yeast was reported (46), but no transcriptional activity was observed in contrast to replication.

Despite the success of the reverse genetics (RG) systems in different animal-infecting NSVs, the *in planta* reconstitution of infectious RNPs for plant-infecting viruses with a segmented RNA genome is particularly difficult. All DNA constructs need to be delivered into the same plant cell, and, for TSWV, the RdRp is exceptionally large (~330 kDa) compared to the RdRp of most other related bunyaviruses (~240 to 260 kDa) and to the typical open reading frames (ORFs) from the plant genome. Expression of such a large protein gene would be very inefficient, and mRNA transcripts from RNA polymerase II transcription of 35S promoter-constructs in the nucleus may also face splicing of cryptic splicing sites. Moreover, achieving the proper ratios of all 3 genome segments in plant cells is not easy or consistent via *Agrobacterium*-mediated delivery of several constructs, and thus affects the outcome of individual experiments. All these obstacles have severely constrained the construction of a reverse genetics system for TSWV in plants.

In this study, we report the complete recovery of infectious TSWV entirely from cDNA clones in plants. The establishment of this reverse genetics system presents the start of a new research era for TSWV and provides a powerful platform to study the basic principles of viral infection cycle and pathogenicity.

Results

Development of a TSWV $S_{(-)}$-Genomic RNA Minireplicon System in *Nicotiana benthamiana*. A minireplicon system based on the S RNA-template was first established before TSWV was rescued entirely from cDNA clones. To this end, a cDNA copy of the TSWV $S_{(-)}$-gRNA was cloned and flanked with a self-cleaving hammerhead (HH) ribozyme at the 5′-terminus and a hepatitis delta virus (HDV) ribozyme at the 3′-terminus. For visual monitoring, quantification purposes, and discrimination between primary and secondary genome transcription, the NSs and N genes were replaced with mCherry and eGFP, respectively (Fig. 1*A*). The resulting $S_{(-)}$ minireplicon reporter was cloned in a binary vector pCB301 downstream of a double 35S promoter (2×35S) and denoted 35S:$SR_{(-)mCherry\&eGFP}$ (Fig. 1*A*). The RdRp and N ORFs were amplified from cDNA of TSWV-infected tissue and cloned into pCambia 2300 binary vector downstream a double 35S promoter. Binary vector constructs of the RdRp, N, and 4 viral RNA silencing suppressor genes (VSRs; P19 from tomato bushy stunt virus [TBSV], HcPro from tobacco etch virus [TEV], and γb from barley stripe mosaic virus [BSMV]; NSs from TSWV) were used to agroinfiltrate *Nicotiana benthamiana* leaves with 35S:$SR_{(-)mCherry\&eGFP}$. The tissues were then monitored for eGFP fluorescence; however, no eGFP fluorescence was observed from 35S:$SR_{(-)mCherry\&eGFP}$ in repeated experiments (*SI Appendix*, Fig. S1*B*).

Because the minireplicon system for TSWV might have failed due to low (unstable) expression of the TSWV RdRp protein, we optimized the codon usage of the RdRp gene for *N. benthamiana* and removed potential intron-splicing sites. The optimized RdRp gene (hereafter RdRp represents optimized RdRp [$RdRp_{opt}$]) was cloned in a binary, 35S-driven expression vector, then used to agroinfiltrate *N. benthamiana* leaves together with binary expression constructs of the N gene, the 4 VSR gene constructs, and the 35S:$SR_{(-)mCherry\&eGFP}$ minireplicon reporter. At 5 d post infiltration (dpi), expression of the reporter genes was analyzed by monitoring the leaves for mCherry and eGFP fluorescence (Fig. 1 *A* and *B*). No fluorescence was observed in the control leaves agroinfiltrated with 35S:$SR_{(-)mCherry\&eGFP}$ alone or coexpressing 35S:$SR_{(-)mCherry\&eGFP}$ with RdRp or N only, whereas eGFP and mCherry fluorescence was consistently observed in leaves agroinfiltrated with 35S:$SR_{(-)mCherry\&eGFP}$ and both N and RdRp (Fig. 1*C*). Expression of the fluorescent reporter proteins was confirmed by Western immunoblot analysis (Fig. 1*D*).

Northern blot analysis showed that both the gRNA and agRNA of the $SR_{(-)mCherry\&eGFP}$ minireplicon were detected in the leaves that coexpressed both N and RdRp at 5 dpi, but not in the leaves coexpressing RdRp or N only (Fig. 1*E*). In addition, using an antisense eGFP probe, we detected genome-length S RNA and subgenomic-sized eGFP mRNA transcripts (Fig. 1 *E*, *Upper*). In a time-course analysis, eGFP and mCherry fluorescence was visible in *N. benthamiana* leaves from 3 dpi onward and gradually increased to 12 dpi (*SI Appendix*, Fig. S2*A*). This was also confirmed by Western immunoblot analysis (*SI Appendix*, Fig. S2*B*).

Altogether, the results indicated that, in *N. benthamiana*, the 35S replicon transcript $SR_{(-)mCherry\&eGFP}$ was properly processed by the HH and RZ and used as a template for replication and transcription of TSWV $S_{(-)}$-gRNA minireplicon by the RdRp. Furthermore, the codon-optimized RdRp was clearly fully functional in supporting viral genome transcription and replication, whereas the wild-type RdRp, for unknown reasons, did not. Somewhat unexpectedly, when the T7 promoter:$SR_{(-)mCherry\&eGFP}$ minireplicon reporter was coexpressed with T7 RNA polymerase, codon-optimized RdRp, N, and 4 VSRs in *N. benthamiana* leaves, no mCherry or eGFP fluorescence was detected (*SI Appendix*, Fig. S1 *A*, *C*, and *D*).

Optimization of the Concentration of N, RdRp, and VSRs on TSWV $SR_{(-)mCherry\&eGFP}$ Minireplicon. Having established a TSWV $S_{(-)}$-gRNA–based minireplicon system in *N. benthamiana*, attempts were made to further optimize the system. To this end, leaves of *N. benthamiana* were agroinfiltrated with binary constructs of the TSWV $S_{(-)}$ minireplicon and varying amounts of N and RdRp gene expression constructs. In these experiments, we increased the concentration of *Agrobacterium* carrying the N expression construct (from OD_{600} 0.2 to 0.8) and kept the level of *Agrobacterium* harboring the RdRp expression construct fixed at OD_{600} 0.2, or vice versa. The results showed the highest eGFP reporter gene expression from the 35S:$SR_{(-)mCherry\&eGFP}$ minireplicon when *Agrobacterium* suspensions bearing N and RdRp expression constructs were both used at OD_{600} 0.2. When *Agrobacterium* harboring either N or RdRp was used at OD_{600} >0.4, the expression of eGFP from the $S_{(-)}$-minireplicon greatly decreased (Fig. 2 *A*–*C*).

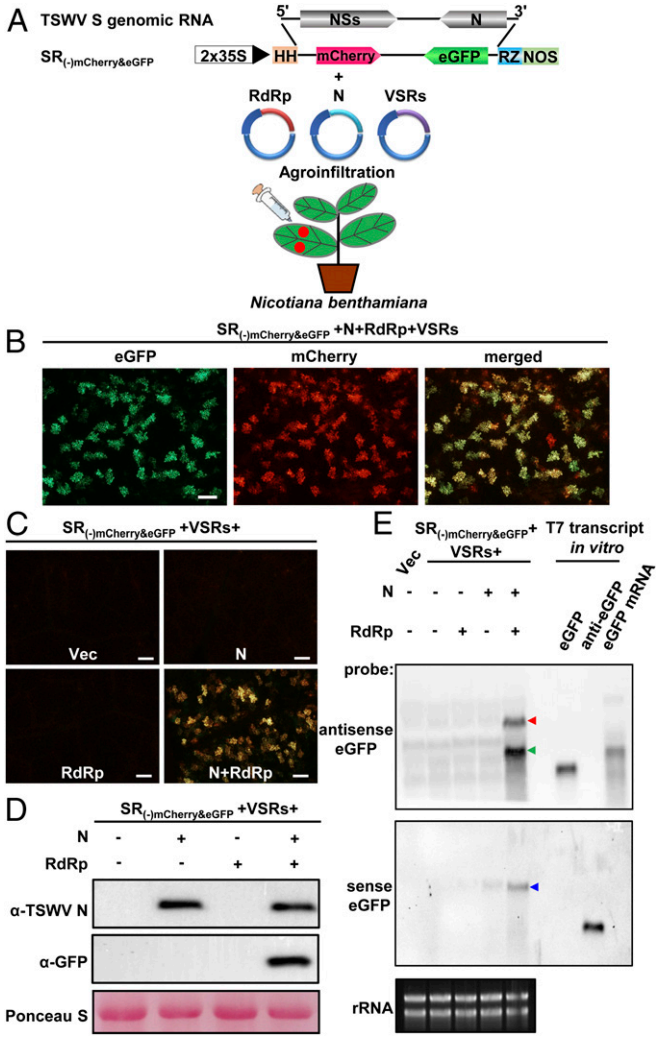

Fig. 1. Construction of TSWV $S_{(-)}$ RNA-based minireplicon system in *N. benthamiana*. (*A*) Schematic representation of binary constructs to express TSWV $S_{(-)}$ minireplicon, TSWV N, RdRp (RdRp representing optimized RdRp), and 4 RNA silencing suppressor (VSRs; NSs, P19, HcPro, and γb) proteins by agroinfiltration into *N. benthamiana*. (*Top*) $S_{(-)}$-gRNA of TSWV. $SR_{(-)mCherry\&eGFP}$: the NSs and N of $S_{(-)}$-gRNA were replaced by mCherry and eGFP, respectively. Minus sign (–) and 5′ to 3′ designation represent the negative (genomic) strand of S RNA; 2×35S, a double 35S promoter; HH, hammerhead ribozyme; RZ, hepatitis delta virus (HDV) ribozyme; NOS, nopaline synthase terminator. (*B*) Foci of eGFP and mCherry fluorescence in *N. benthamiana* leaves coexpressing $SR_{(-)mCherry\&eGFP}$, RdRp, N, and 4 VSRs at 5 d post infiltration (dpi) viewed with a fluorescence microscope. (Scale bar: 400 μm.) (*C*) Analysis of RdRp and N requirement for $SR_{(-)mCherry\&eGFP}$ minigenome replication in *N. benthamiana* leaves. $SR_{(-)mCherry\&eGFP}$ was coexpressed with pCB301 empty vector (Vec), N, RdRp, or both in *N. benthamiana* leaves via agroinfiltration. Agroinfiltrated leaves were examined and photographed at 5 dpi with a fluorescence microscope. Signal shown reflects merged mCherry and eGFP fluorescence from both reporter genes. (Scale bar: 400 μm.) (*D*) Immunoblot analysis of expression of N and eGFP proteins in leaves shown in *C* using specific antibodies against N and GFP, respectively. Ponceau S staining of rubisco large subunit is shown for protein loading control. (*E*) Northern blot analysis of $S_{(-)}$-minireplicon replication and transcription in the presence of N, RdRp, or both in *N. benthamiana*. The S RNA genomic, antigenomic, and subgenomic transcripts (eGFP mRNA) were detected using DIG-labeled sense eGFP or antisense eGFP probes. Red and blue arrows indicate antigenomic and genomic RNAs of $SR_{(-)mCherry\&eGFP}$, respectively. Green arrow indicates eGFP mRNA transcript. Ethidium bromide staining of ribosomal RNA (rRNA) was used as RNA loading control.

Furthermore, at high concentrations ($OD_{600} > 0.6$) of *Agrobacterium*, visible cell death was triggered in the infiltrated leaves (*SI Appendix*, Fig. S3*A*).

Next, in a similar approach, and using the optimized setting, the effects of VSRs on the replication and transcription of the $SR_{(-)mCherry\&eGFP}$ minireplicon were investigated. The 3 VSRs, P19, HcPro, and γb, were shown to yield the highest GFP expression from the SYNV minireplicon when all 3 VSRs were added together (45). Without the addition of VSRs, mCherry and/or eGFP fluorescence was only observed in a small number of cells for the TSWV $SR_{(-)mCherry\&eGFP}$ minireplicon (Fig. 2 *D* and *E*), but these numbers increased with the addition of the 3 VSRs P19, HcPro, and γb (P19-HcPro-γb) or TSWV NSs only (Fig. 2 *D* and *E*). The largest number of cells with eGFP expression from the $S_{(-)}$ minireplicon, as monitored by fluorescence, were obtained when all 4 VSRs (P19-HcPro-γb+NSs) were added (Fig. 2 *D* and *E*). These observations were further confirmed by immunoblot assays (Fig. 2*E*).

Development of a TSWV $S_{(+)}$-agRNA–Based Minireplicon System. For many reverse genetics systems of animal-infecting viruses with negative-stranded/ambisense RNA genomes, minireplicons have initially been established based on gRNA (–). Here, we developed a minireplicon system for TSWV based on agRNA (+). To assess whether the system could be developed based on agRNA, we constructed an $S_{(+)}$-agRNA minireplicon similar to the one based on $S_{(-)}$-gRNA. Within this construct, denoted $SR_{(+)eGFP}$, the N gene was maintained, and only the NSs gene was replaced with eGFP (Fig. 3*A*). Similar to the replicon assays with $SR_{(-)mCherry\&eGFP}$, *N. benthamiana* leaves were agroinfiltrated with binary expression constructs of $SR_{(+)eGFP}$, 4 VSRs, and either N or RdRp separately or together, respectively, and monitored for eGFP fluorescence. No eGFP fluorescence, resulting from primary transcription of the replicon transcript by viral RdRp, was detected when $SR_{(+)eGFP}$ was expressed alone or in the additional presence of N, but eGFP fluoresced when $SR_{(+)eGFP}$ was coexpressed with both RdRp and N and also when $SR_{(+)eGFP}$ was coexpressed with RdRp alone (Fig. 3*B*). These results strongly indicated that a certain (residual) amount of $SR_{(+)eGFP}$ transcripts, resulting from 35S transcription, was not fully processed by the HH and RZ and remained functional in translation, thereby producing N protein. The expression of N protein by $SR_{(+)eGFP}$ was confirmed by Western immunoblot analysis (Fig. 3*C*). Northern blot analysis further showed that samples from the replicon assays in the presence of RdRp and N or RdRp alone contained agRNA, gRNA, and (subgenomic-length) eGFP mRNA transcripts of $SR_{(+)eGFP}$, indicating the occurrence of replication and transcription (Fig. 3*D*). Altogether, these results demonstrate that the N protein can also be expressed from the $SR_{(+)eGFP}$ replicon to support its transcription and replication. This system thus provides an attractive alternative to the $S_{(-)}$-gRNA–based minireplicon because additional binary expression constructs for N do not have to be supplied.

Development of an $M_{(-)}$-gRNA–Based Minireplicon for Cell-to-Cell Movement of TSWV in *N. benthamiana*. As a first step toward developing a reverse genetics system to rescue TSWV virus entirely from cDNA, a movement-competent minireplicon was also established. To this end, a minireplicon based on TSWV $M_{(-)}$-gRNA was constructed, similar to the ones made for $S_{(-)}$ and $S_{(+)}$. Within this construct, the NSm cell-to-cell movement protein gene was maintained, but the GP ORF was exchanged for eGFP, resulting in a minireplicon, designated as $MR_{(-)eGFP}$ (Fig. 4*A*). After *Agrobacterium*-mediated delivery of the construct into *N. benthamiana*, no eGFP fluorescence was observed in leaves containing the $MR_{(-)eGFP}$ replicon with RdRp or N. However, in the presence of both RdRp and N, eGFP fluorescence was expressed in a group of cells adjacent to each other

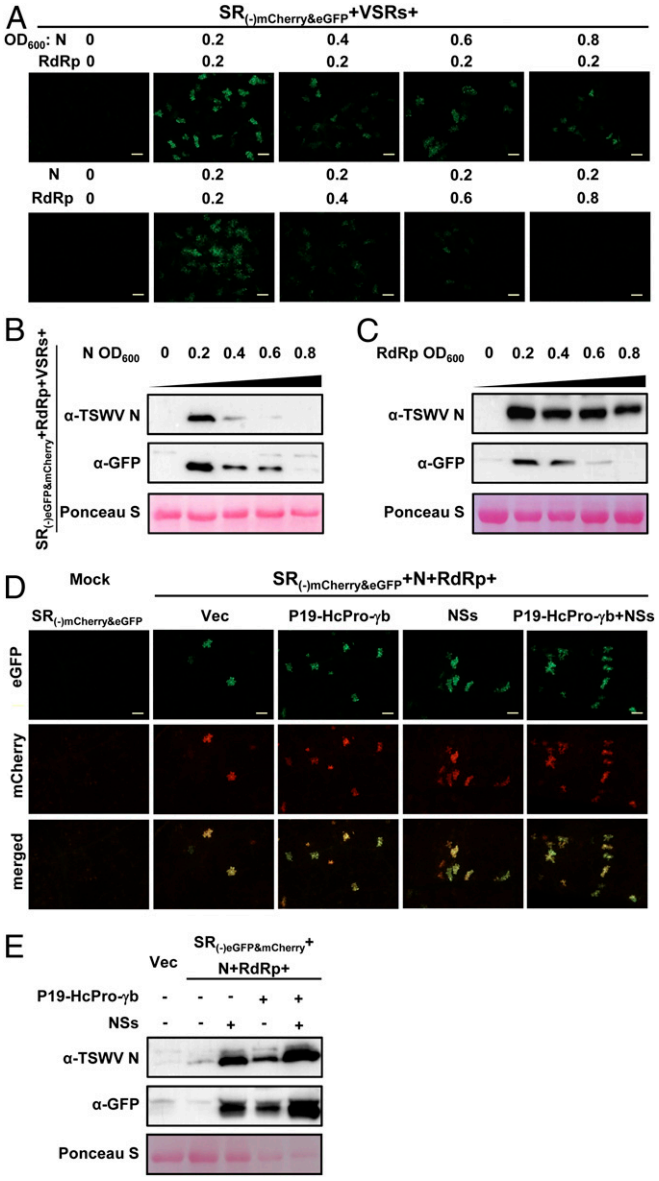

Fig. 2. Optimization of $SR_{(-)mCherry\&eGFP}$ minireplicon system. (*A*) Optimizing the concentration of N and RdRp proteins for replication and transcription of $SR_{(-)mCherry\&eGFP}$ in *N. benthamiana* leaves. Increasing amounts of *Agrobacterium*, from OD_{600} = 0.2 to 0.8 and containing the binary expression constructs for N (*Upper*) or RdRp (*Bottom*), were mixed with fixed amounts of *Agrobacterium* containing the RdRp or N construct (OD_{600} 0.2), respectively; their effects on eGFP reporter expression were visualized with a fluorescence microscope at 5 dpi. (Scale bars: 400 μm.) (*B* and *C*) Western immunoblot detection of the N and eGFP proteins expressed in the leaves shown in *A* using specific antibodies against N and GFP, respectively. (*D*) Optimization of RNA silencing suppressors (VSRs) on $SR_{(-)mCherry\&eGFP}$ mini-reporter replication and transcription as measured by eGFP and mCherry expression. The $SR_{(-)mCherry\&eGFP}$, N, and RdRp proteins were coexpressed with pCB301 empty vector (Vec), NSs, P19-HcPro-γb, or all 4 VSRs in *N. benthamiana* leaves. Foci expressing eGFP and mCherry in agroinfiltrated leaves were visualized with a fluorescence microscope at 5 dpi. (Scale bars: 400 μm.) (*E*) Western immunoblot detection of N and eGFP protein synthesis in the leaves shown in *D* using N- and GFP-specific antibodies, respectively. Ponceau S staining was used as protein loading control.

(Fig. 4 *B* and *C*). In comparison to the eGFP fluorescence from the $SR_{(-)mCherry\&eGFP}$ or the $SR_{(+)eGFP}$ reporter that always expressed in single plant cells, the results suggested that the $MR_{(-)eGFP}$ minireplicon had moved from cells to cells in *N. benthamiana* leaves. Northern blot analysis confirmed the synthesis of gRNA, agRNA, and (subgenomic-length) eGFP mRNA transcripts of the $MR_{(-)eGFP}$ replicon in the presence of both RdRp and N, but not with RdRp or N only (Fig. 4*D*).

To further substantiate the findings on possible cell-to-cell movement of the $MR_{(-)eGFP}$ minireplicon, a stop codon was introduced immediately downstream of the start codon of NSm, and the construct was designated as $MR_{(-)eGFP\&NSmMut}$ (Fig. 4*A*). When the $MR_{(-)eGFP\&NSmMut}$ replicon was delivered and coexpressed with RdRp and N in *N. benthamiana* leaves, eGFP fluorescence was only detected in single cells (Fig. 4*B*). As expected, Western immunoblot analysis confirmed the production of eGFP protein in leaves containing the $MR_{(-)eGFP\&NSmMut}$ replicon and in significantly lower amounts compared to the $MR_{(-)eGFP}$ replicon (Fig. 4*C*).

Establishment of Systemic Infection of $M_{(-)}$- and $S_{(+)}$-Minireplicon Reporters by Coexpression of Full-Length Antigenomic $L_{(+)}$ in *N. benthamiana*. With the S (g/ag)RNA-based minireplicon systems and a movement-competent M gRNA-based minireplicon established, we set out to construct full-length genomic cDNA clones of $L_{(-)}$, $M_{(-)}$, and $S_{(-)}$, flanked by HH and HDV ribozymes at the 5′- and 3′-terminus, as a first step toward the rescue of TSWV entirely from cDNA clones. At the same time, similar constructs were made for the antigenomic $L_{(+)}$, $M_{(+)}$, and $S_{(+)}$.

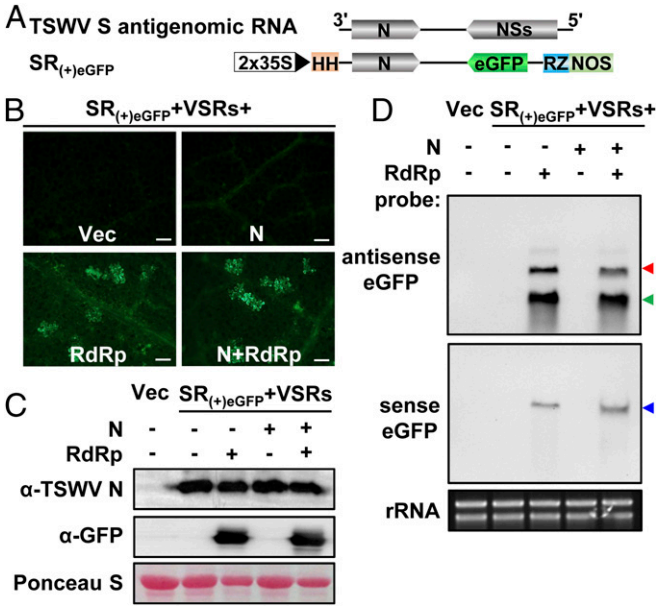

Fig. 3. Development of $S_{(+)}$-agRNA minireplicon system in *N. benthamiana*. (*A*) Schematic representation of the TSWV $SR_{(+)eGFP}$ minireplicon. Plus sign (+) and 3′ to 5′ designation represent the positive (antigenomic) strand of S RNA. The NSs gene of TSWV S antigenomic RNA was replaced by eGFP. Antigenomic RNA strands of the $SR_{(+)eGFP}$ minireplicon are transcribed from a double 35S promoter (2×35S) and flanked by an HH ribozyme and HDV ribozyme (RZ) sequence. (*B*) Foci of eGFP fluorescence in *N. benthamiana* leaves coexpressing TSWV $SR_{(+)eGFP}$ with pCB301 empty vector (Vec), N, RdRp, or N+RdRp by agroinfiltration. Agroinfiltrated leaves were photographed at 3 dpi using a fluorescence microscope. (Scale bars: 400 μm.) (*C*) Western immunoblot detection of N and eGFP protein synthesis in the leaves shown in *B* using N- and GFP-specific antibodies, respectively. Ponceau S staining was used as a protein loading control. (*D*) Northern blot analysis of the replication and transcription of $SR_{(+)eGFP}$ minireplicon in *N. benthamiana* coexpressed with empty vector (Vec), N, RdRp, or both. Genomic RNAs (red arrow), antigenomic RNAs (blue arrow), and subgenomic-length eGFP mRNA transcripts (green arrow) were detected with DIG-labeled sense and antisense eGFP probes, respectively. Ethidium bromide staining was used as RNA loading control.

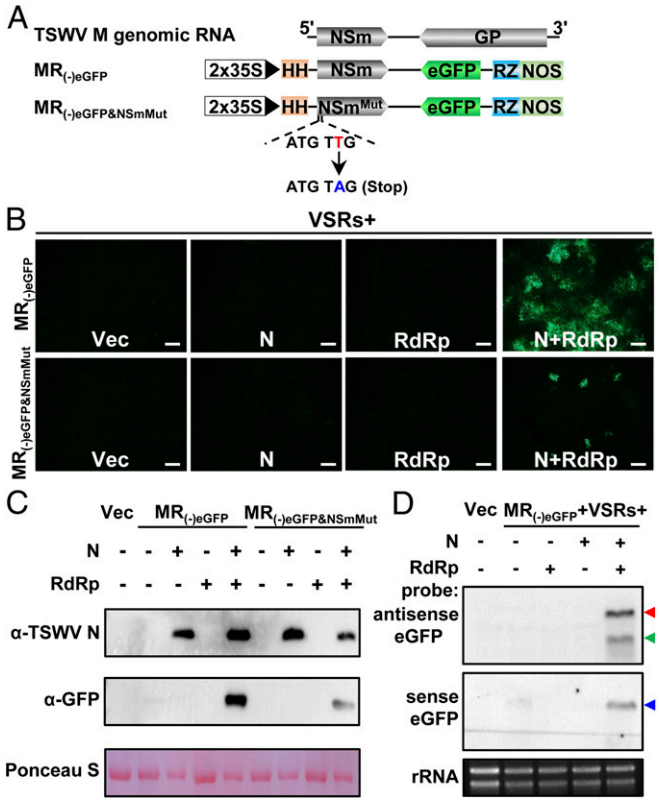

Fig. 4. Establishment of TSWV $M_{(-)}$-gRNA–based minireplicon system with cell-to-cell movement competency in *N. benthamiana*. (*A*) Schematic representation of the TSWV $MR_{(-)eGFP}$ minireplicon and its mutant derivative $MR_{(-)eGFP\&NSmMut}$. Minus sign (–) and 5′ to 3′ designation represent the genomic RNA of TSWV M. The GP gene of TSWV $M_{(-)}$ gRNA was replaced with eGFP. Genomic RNA of the minireplicon is transcribed from a double 35S promoter (2×35S) and flanked by a hammerhead (HH) ribozyme and HDV ribozyme (RZ). For $MR_{(-)eGFP\&NSmMut}$, a stop codon was introduced immediately after the start codon of the NSm gene in the $MR_{(-)eGFP}$ minireplicon. (*B*) Foci of eGFP fluorescence expressed from the $MR_{(-)eGFP}$ or $MR_{(-)eGFP\&NSmMut}$ minireplicon in *N. benthamiana* leaves coexpressed with the empty vector (Vec), N, RdRp, or N+RdRp by agroinfiltration. Agroinfiltrated leaves were photographed at 4 dpi with a fluorescence microscope. (Scale bars: 400 μm.) (*C*) Western immunoblot detection of N and eGFP protein synthesis in the leaves shown in *B* with specific antibodies against N and GFP, respectively. Ponceau S staining was used as protein loading control. (*D*) Northern blot analysis of replication and transcription of the $MR_{(-)eGFP}$ minireplicon coexpressed with Vec, N, RdRp, or N+RdRp in *N. benthamiana* leaves. Antigenomic RNAs (red arrow), genomic RNAs (blue arrow), and eGFP mRNA transcripts (green arrow) were detected with DIG-labeled sense and antisense eGFP probes, respectively. Ethidium bromide staining was used as RNA loading control.

However, all attempts to recover infectious TSWV from *N. benthamiana* after agrobacterium-mediated delivery of all binary expression constructs of the genomic $L_{(-)}$, $M_{(-)}$, and $S_{(-)}$ together with N, RdRp, and 4 VSRs, and also with the antigenomic $L_{(+)}$, $M_{(+)}$, and $S_{(+)}$ constructs, failed (Table 1).

Since $MR_{(-)eGFP}$ was shown earlier to be movement-competent, we next investigated whether the $M_{(-)}$- and $S_{(-)}$-minigenomes moved into the same plant cell in the presence of both RdRp and N. Upon coexpression of $MR_{(-)mCherry}$, $SR_{(-)eGFP}$, RdRp, and N in *N. benthamiana* leaves, expression of both mCherry and eGFP from the $MR_{(-)mCherry}$ and $SR_{(-)eGFP}$ minireplicons, respectively, could be discerned. However, the foci of mCherry fluorescence were separated from those with eGFP fluorescence (*SI Appendix*, Fig. S3*B*). The results suggested that the ectopic expression of TSWV RdRp and N might interfere with and block intercellular movement of $SR_{(-)eGFP}$ into cells containing $MR_{(-)mCherry}$. To avoid that interference, a different strategy was used in which RdRp and N were expressed from viral agRNAs. To this end, we made a construct of the full-length L agRNA containing the optimized RdRp and flanked by the HH and HDV ribozymes, denoted $L_{(+)opt}$ (Fig. 5*A*). To test the expression and functionality of RdRp from this construct, $L_{(+)opt}$ was coexpressed with the $SR_{(-)mCherry\&eGFP}$ minireplicon, N, and VSRs in *N. benthamiana* leaves. The results showed clear eGFP and mCherry fluorescence and indicated that $L_{(+)opt}$ was able to support $SR_{(-)mCherry\&eGFP}$ transcription and replication (*SI Appendix*, Fig. S4*A*). Furthermore, $L_{(+)opt}$ was also able to support the replication and transcription of the $SR_{(+)eGFP}$ minireplicon, without the additional ectopic expression of N (*SI Appendix*, Fig. S4*B*), and of the movement-competent $MR_{(-)eGFP}$ (*SI Appendix*, Fig. S4*C*).

In the next experiment, $L_{(+)opt}$ was coexpressed with $MR_{(-)mCherry}$, $SR_{(+)eGFP}$, and 4 VSRs in *N. benthamiana*, and plants were then analyzed for systemic infection (Fig. 5*A*). At 6 dpi, mCherry and eGFP fluorescence was detected in the locally agroinfiltrated *N. benthamiana* leaves, and some foci expressed mCherry and eGFP together (*SI Appendix*, Fig. S5*A*). At 15 dpi, necrotic symptoms were visible in systemic leaves of *N. benthamiana* (Fig. 5 *B*, *a* and *c*). In leaves exposed to a handheld UV lamp, distinct eGFP fluorescence was also observed in those leaves (Fig. 5 *B*, *b* and *d*). The eGFP signal was detected in 24 of 30 agroinfiltrated *N. benthamiana* plants (Table 1). Both eGFP and mCherry fluorescence were visible with a fluorescence microscope in veins/stems and systemically infected leaves (Fig. 5 *B*, *e*). The systemic infection of *N. benthamiana* with $SR_{(+)eGFP}$, $MR_{(-)mCherry}$, and $L_{(+)opt}$ was further confirmed by RT-PCR analysis (*SI Appendix*, Fig. S5*B*). Thus, systemic infection with the TSWV $SR_{(+)eGFP}$- and $MR_{(-)mCherry}$-minireplicon reporters was established by coexpression of full-length antigenomic $L_{(+)opt}$ in *N. benthamiana* plants, despite the TSWV-derivative mutant neither encoding the silencing suppressor NSs nor encoding GP.

Recovery of Infectious TSWV from the Full-Length cDNA Clones. Based on the establishment of the systemic infection after *Agrobacterium*-mediated delivery of replicons $SR_{(+)eGFP}$, $MR_{(-)mCherry}$, and $L_{(+)opt}$, we next generated a full-length construct for S agRNA without any reporter gene, designated as $S_{(+)}$, for coexpression with replicon constructs $L_{(+)opt}$, $M_{(-)}$, and 4 VSRs in *N. benthamiana* leaves. However, and surprisingly, no infectious TSWV was recovered from systemic leaves of *N. benthamiana* that were infiltrated with these constructs (Table 1). To find out whether this was due to failure of $S_{(+)}$, we next examined whether $S_{(+)}$ was able to establish a systemic infection in combination with the functional $MR_{(-)eGFP}$ and $L_{(+)opt}$ constructs. When $L_{(+)opt}$, $MR_{(-)eGFP}$, $S_{(+)}$, and 3 VSRs (P19-HcPro-γb) were coexpressed in *N. benthamiana* leaves, eGFP fluorescence was visible at 18 dpi in systemically infected leaves of *N. benthamiana* (Fig. 5*D*). However, only 7 of 60 plants showed systemic infection for the full-length $S_{(+)}$ compared to 24 of 30 plants with the $SR_{(+)eGFP}$ replicon (Table 1). RT-PCR analysis confirmed the systemic infection with $S_{(+)}$, $MR_{(-)eGFP}$, and $L_{(+)opt}$ in those *N. benthamiana* (*SI Appendix*, Fig. S5*C*). When $L_{(+)opt}$, $MR_{(-)eGFP}$, and $S_{(+)}$ were coexpressed with 4 VSRs (P19-HcPro-γb and NSs) in *N. benthamiana* leaves, intriguingly, no eGFP fluorescence was observed in the systemically infected leaves (Table 1), suggesting that ectopic expression of NSs interfered with the rescue of the virus from the full-length $S_{(+)}$, $MR_{(-)eGFP}$, and $L_{(+)opt}$.

Next, we tested for rescue of the virus from the full-length $M_{(-)}$, $SR_{(+)eGFP}$, and $L_{(+)opt}$. To this end, the $L_{(+)opt}$, $M_{(-)}$, and $SR_{(+)eGFP}$ constructs were delivered to and coexpressed in *N. benthamiana* in the presence of either 4 (P19-HcPro-γb+NSs) or 3 (P19-HcPro-γb) VSRs. The results showed no eGFP fluorescence in systemically infected leaves of *N. benthamiana* at 15 to 50 dpi, indicating that $M_{(-)}$ was not able to complement and rescue the $S_{(+)}$-minireplicons into systemically infected leaves

Table 1. Systemic infection rate of recombinant TSWV rescued in *N. benthamiana* in the presence of viral suppressors of RNA silencing (VSRs)

Genome and antigenome derivatives	VSRs	No. of infected plants/inoculated plants	Systemically infected plants, %
$S_{(-)}$+$M_{(-)}$ +$L_{(-)}$	N+RdRp+NSs+P19-HcPro-γb	0/30	0
$S_{(+)}$+$M_{(+)}$+$L_{(+)}$	N+RdRp+NSs+P19-HcPro-γb	0/30	0
$SR_{(+)eGFP}$+$MR_{(-)mCherry}$+$L_{(+)opt}$	NSs+P19-HcPro-γb	24/30	80
$S_{(+)}$+$MR_{(-)eGFP}$+$L_{(+)opt}$	P19-HcPro-γb	7/60	11.37
$S_{(+)}$+$MR_{(-)eGFP}$+$L_{(+)opt}$	NSs+P19-HcPro-γb	0/60	0
$SR_{(+)eGFP}$+$M_{(-)}$+$L_{(+)opt}$	P19-HcPro-γb	0/60	0
$SR_{(+)eGFP}$+$M_{(-)}$+$L_{(+)opt}$	NSs+P19-HcPro-γb	0/60	0
$SR_{(+)eGFP}$+$M_{(-)opt}$+$L_{(+)opt}$	NSs+P19-HcPro-γb	27/30	90
$S_{(+)}$+$M_{(-)}$+$L_{(+)opt}$	NSs+P19-HcPro-γb	0/60	0
$S_{(+)}$+$M_{(-)opt}$+$L_{(+)opt}$	P19-HcPro-γb	6/60	10

Mixture of *Agrobacterium* cultures harboring the plasmids encoding each of the S, M, L, and derivatives (final concentration, OD_{600} = 0.2), RdRp (OD_{600} = 0.2), N (OD_{600} = 0.2), and VSRs (OD_{600} = 0.05) were used to infiltrate *N. benthamiana* leaves. Systemic infection was scored at 15 to 30 dpi.

(Table 1). Northern blot analysis showed that neither gRNAs nor agRNAs were detected for $M_{(-)}$, while, in contrast, gRNAs and agRNAs were detected for $S_{(+)}$ (*SI Appendix*, Fig. S6 *A* and *B*). Earlier, the $MR_{(-)eGFP}$ minireplicon was shown to replicate and be transcribed (Fig. 4*D*). The only difference between the $M_{(-)}$ and $MR_{(-)eGFP}$ minireplicons was the GP gene, which was exchanged for eGFP in the second construct. Considering that primary $M_{(-)}$ transcripts were produced in the nucleus by the 35S promoter and putative splice sites were also predicted in the GP sequence (*SI Appendix*, Table S2), it was likely that the primary $M_{(-)}$ transcripts were prone to splicing before sufficient replication of the minireplicon and transcriptional-translational expression of the cell-to-cell movement protein gene could take place. For this reason, codon optimization was performed on the GP gene sequence in $M_{(-)}$, leading to a new construct designated as $M_{(-)opt}$ (Fig. 5*A*). Upon coexpression of $L_{(+)opt}$, $M_{(-)opt}$, and $SR_{(+)eGFP}$ minireplicon in *N. benthamiana*, eGFP fluorescence was observed in systemically infected leaves (Fig. 5*C*). Fluorescence was observed in 27 of 30 agroinfiltrated plants, demonstrating that $M_{(-)opt}$ produced a functional and stable M genomic RNA, able to replicate and support systemic movement of S and L RNP molecules by its encoded NSm protein (Table 1). RT-PCR analysis further confirmed systemic infection of *N. benthamiana* with $SR_{(+)eGFP}$, $M_{(-)opt}$, and $L_{(+)opt}$ (*SI Appendix*, Fig. S5*D*).

In a final experiment, aiming to rescue "wild-type" TSWV entirely from cDNA clones, the binary constructs of $L_{(+)opt}$, $M_{(-)opt}$, and $S_{(+)}$ were agroinfiltrated with 3 VSRs (P19-HcPro-γb) into *N. benthamiana* leaves. At 19 dpi, typical leaf curling was observed in systemically infected leaves from *N. benthamiana* plants (Fig. 6*A* and Table 1). As the disease progressed, the stunted phenotype was observed between 19 and 30 dpi. When the experiment was repeated with more plants, symptoms of systemic infection were observed in 6 of 60 plants (Table 1). Northern blot analyses on samples collected from systemically infected leaves showed the presence of gRNA and agRNA of S, M, and L RNA segments (Fig. 6*B*), which was also confirmed by RT-PCR (*SI Appendix*, Fig. S7). The subgenomic RNA of S and M RNA segments was also detected (Fig. 6*B*). Moreover, sequence analysis of the amplicons derived from the L and M RNA confirmed the presence of codon-optimized RdRp and GP gene sequences (Fig. 6*C*). Immunoblot analysis of systemically infected leaf samples showed the presence of N, NSs, NSm, Gn, and Gc proteins in *N. benthamiana* (Fig. 6*D*), altogether indicating successful systemic infection with rescued TSWV (rTSWV).

To demonstrate genuine virus particle rescue of rTSWV, we subjected samples from newly infected systemic leaf tissues to transmission electron microscopy (TEM). As shown in Fig. 6 *E* and *F*, typical enveloped and spherical virus particles were observed in rTSWV-infected tissue. The immunogold labeling of TEM sections using a gold-labeled anti-Gn antiserum showed that the rTSWV particles were labeled with the immunogold particles (Fig. 6 *G* and *H*).

Collectively, infectious TSWV was successfully rescued from full-length cDNA clones of $L_{(+)opt}$, $M_{(-)opt}$, and $S_{(+)}$.

Discussion

The establishment of a reverse genetics system for a segmented NSV basically requires 2 steps. The first involves in vivo reconstitution of transcriptionally active RNPs, often managed by development of a minigenome replication system. The second step involves virus rescue entirely from full-length infectious cDNA clones, based on tools developed and optimized with the minigenome replication system. In this study, we first successfully reconstituted infectious RNPs based on TSWV $S_{(-)}$-gRNA and $S_{(+)}$-agRNA after optimizing the sequence of RdRp. Next, a movement-competent minigenome replication system was developed based on $M_{(-)}$-gRNA, which was also able to complement and systemically rescue reconstituted S RNPs. In a third step, full-length constructs were made for $S_{(+)eGFP}$-agRNA, $M_{(-)mCherry}$-gRNA, and $L_{(+)opt}$-agRNA to directly accommodate translation of (small amounts of) all 3 genomic (35S) transcripts into N, NSm, and RdRp proteins, respectively, and avoid the additional need of ectopically expressed N and RdRp. *Agrobacterium*-mediated delivery of these constructs led to systemic infection of *N. benthamiana* with rTSWV carrying eGFP reporters. In a last step, the GP gene sequence of $M_{(-)}$ was optimized, which allowed the final rescue of infectious rTSWV particles entirely from full-length cDNA clones in *N. benthamiana*.

The choice of plant promoter to generate the first primary full-length genomic RNA template (mimicking authentic genomic RNA molecules) for initiating viral replication is one of the major and critical factors for the construction of a reverse genetics system for TSWV. The genomic RNAs of segmented NSVs contain highly conserved sequences at their 5′ and 3′ termini that show inverted sequence complementarity and fold into the panhandle structure that has a major role in RNA transcription and replication. Any additional nucleotide residues at those termini in the past have been shown to disrupt/affect transcription-replication of animal-infecting segmented NSVs (47). Moreover, the genomic RNAs of segmented NSVs possess neither a 5′-cap structure nor 3′-poly(A) tail (2, 48). Therefore, the promoter used should also generate transcripts to meet those requirements. For animal-infecting segmented NSVs, researchers have used various systems. One of the first strategies employed bacteriophage

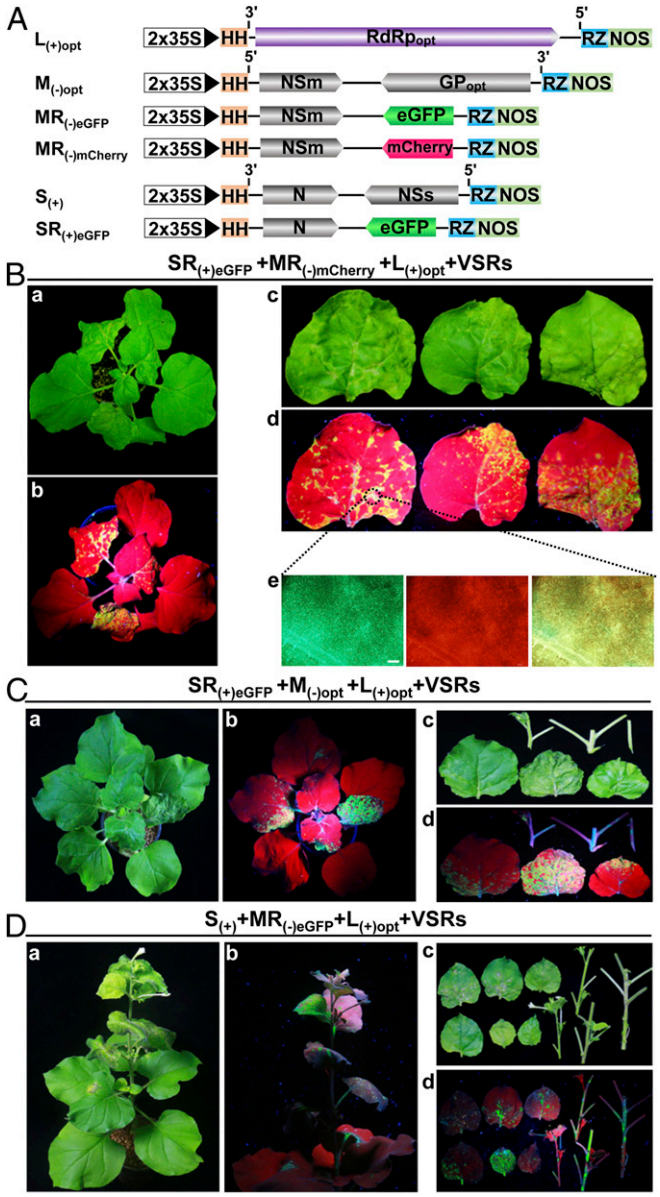

Fig. 5. Establishment of systemic infection in *N. benthamiana* with replicons $S_{(+)}$ and $M_{(-)}$ coexpressed with full-length antigenomic $L_{(+)opt}$. (*A*) Schematic representation of constructs expressing TSWV full-length antigenomic $L_{(+)opt}$ with optimized RdRp ($RdRp_{opt}$), full-length genomic $M_{(-)opt}$ with optimized GP (GP_{opt}), $MR_{(-)eGFP}$, $MR_{(-)mCherry}$, full-length antigenomic $S_{(+)}$, and $SR_{(+)eGFP}$. Plus sign (+) and 3′ to 5′ designation represent the antigenomic RNA of TSWV; minus sign (–) and 5′ to 3′ designation represent the genomic RNA of TSWV. Primary viral RNA transcripts are transcribed from a double 35S promoter (2×35S) and flanked by an HH and HDV ribozyme (RZ). (*B*) eGFP and mCherry fluorescence in *N. benthamiana* resulting from systemic infection of agroinfiltrated $SR_{(+)eGFP}$, $MR_{(-)mCherry}$, and $L_{(+)opt}$ constructs. Systemically infected plants (a and b) and leaves (c and d) were photographed at 21 dpi under white light and (hand-held) ultraviolet (UV) light. Foci of eGFP and mCherry fluorescence in leaves shown in d as visualized with a fluorescence microscope (e). (Scale bar: 400 μm.) (*C*) eGFP fluorescence in *N. benthamiana* resulting from systemic infection with agroinfiltrated $SR_{(+)eGFP}$, $M_{(-)opt}$, and $L_{(+)opt}$ constructs. Infected plants (a and b) and leaves (c and d) were photographed at 18 dpi under white light and (hand-held) UV light, respectively. (*D*) eGFP fluorescence in *N. benthamiana* resulting from systemic infection of agroinfiltrated $S_{(+)}$, $MR_{(-)eGFP}$, and $L_{(+)opt}$ constructs. Infected plants (a and b) and leaves (c and d) were photographed at 50 dpi under white light and (hand-held) UV light, respectively.

T7 promoter constructs coexpressed with a T7 RNA polymerase, and, later, RNA polymerase I (Pol I) promoter constructs were used to generate uncapped genomic RNAs that can serve as the initial template for replication in mammalian cells (42, 43, 49–51). Unfortunately, attempts to establish the TSWV minireplicon system using the same T7 promoter and T7 RNA polymerase strategy that are available to animal virologists were unsuccessful (*SI Appendix*, Fig. S1 *A*, *C*, and *D*). The Pol I promoter was not characterized well in plants and has never been used to rescue plant viruses from cDNA clones. Although a Pol I promoter has been reported from *Arabidopsis* (52, 53), the transcription initiation +1 site is still not known. The 35S promoter, an RNA Pol II promoter, is well characterized and hence remains the only choice to establish a reverse genetics system for TSWV in plants. The Pol II promoter, which generates transcripts containing the 5′ cap-structure, has been used to produce the initial viral RNA transcripts of an animal-infecting nonsegmented NSV (54). The 35S/Pol II promoter was also used to produce a primary viral RNA template of the first nonsegmented plant NSV reconstituted, the SYNV rhabdovirus (11, 45). However, for the construction of reverse genetics of segmented NSVs in animal cells, all animal-infecting viruses have been reconstituted using T7/Pol I promoter-driven production of primary viral RNA templates for replication. Here, we successfully deployed the 35S/Pol II promoter and 2 ribozymes at the 5′ and 3′ ends of viral RNA sequences to generate full-length viral RNA transcripts that are recognized as initial/"authentic" RNA templates for TSWV replication and transcription by viral N and RdRp. Whereas animal virologists have used cell culture systems to rescue the virus (42–44, 50, 55, 56), here we rescued TSWV in whole plants.

In addition to the promoter, the RdRp protein may present another bottleneck for the establishment of a reverse genetics system. Tospoviruses code for a single, unprocessed ∼330-kDa RdRp from the 8.9-kb-sized L RNA (20, 21). The RdRp gene sequence of TSWV was predicted to contain numerous intron-splicing sites (*SI Appendix*, Table S1). Since the first segmented negative-stranded animal RNA virus was rescued in 1996 (42), numerous groups worldwide have attempted to construct a reverse genetics system for a tospovirus in plants but all have failed. Here, we have shown that codon optimization and removal of potential intron-splicing sites were crucial for the expression of a functional RdRp of tospovirus from 35S-driven constructs in planta (Fig. 1*B*). While codon optimization may have contributed to increased protein expression levels, removal of predicted potential intron-splicing sites from the RdRp gene may have helped to further stabilize and increase expression levels. After all, TSWV is known to replicate in the cytoplasm (2, 48), and its RdRp gene may not have evolved to escape from the nuclear (pre-mRNA) splicing machinery. After nuclear transcription of the RdRp gene by the 35S promoter, any intron-splicing site in the wild-type RdRp transcript could thus result in a truncated, nonfunctional RdRp.

In addition to being crucial for RdRp, an optimized GP gene sequence also turned out to be crucial to rescue a full-length M RNA-based transcriptionally active RNP. Whereas the $M_{(-)mCherry}$ minireplicon was able to establish systemic infection in *N. benthamiana* when coexpressed with $S_{(+)eGFP}$ minireplicon and $L_{(+)opt}$, the wild-type full-length M segment was not. As in the case with the RdRp gene sequence, the GP gene sequence of TSWV was also predicted to contain numerous intron-splicing sites (*SI Appendix*, Table S2). The absence of antigenomic and genomic RNA strands from the wild-type full-length M replicon on Northern blots (*SI Appendix*, Fig. S6*B*) indicated the possibility that primary transcripts could have been prone to splicing in the GP sequence. Splicing of the M segment would not only lead to a loss of genome-length RNA molecules, but also inhibit the production of NSm protein (either from direct translation of the primary M transcript or after secondary transcription of

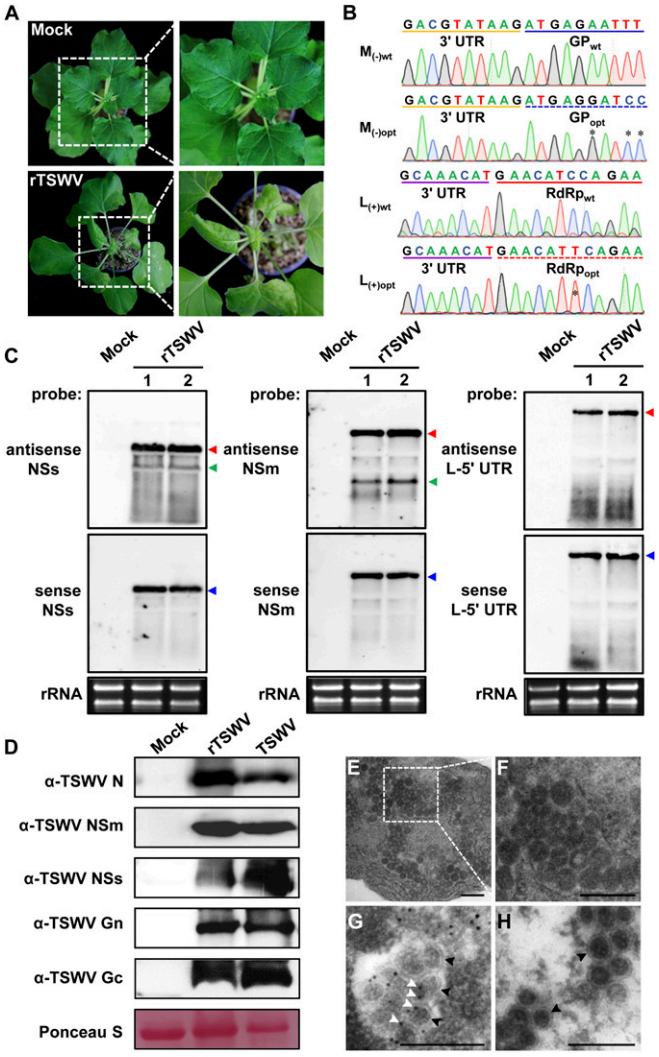

Fig. 6. Rescue of infectious TSWV from full-length cDNA clones in *N. benthamiana*. (*A*) Systemic infection of *N. benthamiana* plants with rescued TSWV (rTSWV) resulting from agroinfiltration of $S_{(+)}$, $M_{(-)opt}$, and $L_{(+)opt}$ and 3 VSRs (P19, HcPro, and γb). The plant agroinfiltrated with pCB301 empty vector was used as a mock control. Images were taken at 19 dpi. Boxed areas (*Left*) of the plants that show stunting, mosaic, and leaf curling are shown enlarged (*Right*). (*B*) Sequence confirmation of codon-optimized sequences of GP gene [from $M_{(-)opt}$ RNA segment] and RdRp gene [from the $L_{(+)opt}$ RNA segment] on RT-PCR fragments obtained from systemic leaves of *N. benthamiana* infected with rTSWV. The optimized sequence of GP from rTSWV is underlined with a blue dashed line; wild-type GP sequence is underlined in blue. The 3′-untranslated region (UTR) sequence of the M genomic RNA is marked with a yellow line. The optimized sequence of RdRp from rTSWV is underlined with a red dashed line, and wild-type RdRp sequence is underlined in red. The 3′-UTR sequence of the L genomic RNA is marked with a purple line. The stars indicate codon-optimization sites of GP and RdRp gene sequences. (*C*) Northern blot detection of viral RNA from the S, M, and L RNA segment, respectively, in systemically leaves of *N. benthamiana* infected with rTSWV. Genomic RNAs (red arrow), antigenomic RNAs (blue arrow), and subgenomic RNAs (green arrow) were detected with DIG-labeled sense and antisense NSs-, NSm-, and L-5′ UTR probes, respectively. Lanes 1 and 2 refer to 2 independent replicates. Ethidium bromide staining was used as RNA loading control. (*D*) Western immunoblot detection of the viral proteins from leaves systemically infected with rTSWV using specific antibodies against N, NSm, NSs, Gc, and Gn, respectively. Leaves infected with wild-type TSWV were used as a positive control. Ponceau S staining was used as protein loading control. (*E* and *F*) Electron micrographs of thin sections of *N. benthamiana* plants infected with rTSWV (*E*). Boxed regions (*E*) show virions and are also shown enlarged (*F*). (*G*) Immunogold labeling of spherical, enveloped virus particles with anti-serum against Gn followed by a goat anti-rabbit Immunoglobulin G (IgG) conjugated with gold particles. (*H*) Immunogold labeling of virus particles using only the goat anti-rabbit IgG conjugated with gold particles. White arrowheads indicate gold particles; black arrowheads indicate spherical, enveloped virus particles. (Scale bars: 0.2 μm.)

NSm mRNA) needed for cell-to-cell and systemic movement of viral RNPs.

Not only the wild-type sequence of L and M RNA segments may be spliced in the nucleus; the S RNA segment generated by the 35S promoter could also be prone to splicing. This possibility is supported by the experiments in which *N. benthamiana* was infiltrated with the $S_{(+)eGFP}$ minireplicon, $M_{(-)opt}$, and $L_{(+)opt}$, which resulted in 80% virus recovery (Table 1), but, when only the $S_{(+)eGFP}$ minireplicon was exchanged for the full-length $S_{(+)}$, virus recovery dropped to 11.37%. Cryptic site splicing may also explain the low infection rate (10%) when full-length $S_{(+)}$, $M_{(-)opt}$, and $L_{(+)opt}$ were coexpressed (Table 1). Although this could be due to the splicing of S RNA, the (residual) levels of the full-length S produced apparently were sufficient to initiate viral replication.

Similar to the case in other bunyaviruses (42, 51, 57), both the RdRp and N proteins are absolutely required for reconstitution of infectious RNPs complexes for TSWV. In the minireplicon system, an ectopic supply of N and RdRp proteins is essential for supporting the replication and transcription of TSWV S- and M-minireplicon (Fig. 1*C*). However, high expression of either N or RdRp results in cell death and reduced the eGFP expression from TSWV minireplicon. Moreover, in our attempts to rescue TSWV from full-length cDNA clones, ectopic expression of N and RdRp intriguingly interfered with the progeny L-, M-, and S-RNA segments moving into neighboring plant cells that already contain 1 or 2 RNA segments of L, M, and S. The presence of L-, M-, and S- RNA segments in the same cells, however, is a prerequisite for the reconstitution of infectious TSWV and for systemic spread in *N. benthamiana.* Fortunately, direct expression of N from $S_{(+)}$ and RdRp from $L_{(+)opt}$ led to recovery of the infectious TSWV. Whether this virus recovery is due to the fact that N and RdRp are directly expressed from primary viral genome transcripts and simultaneously associate with progeny L-, M-, and S-RNA segments in the same plant cells into infectious RNPs and/or it involves a more fine-tuned protein expression relative to RNA segment replication remains unclear.

The TSWV-derivative mutant that does not encode the RNA silencing suppressor NSs is still able to systemically infect the *N. benthamiana* plant (Fig. 5 *A* and *B*). This result is consistent with early reports that TSWV coding for a truncated NSs that no longer has RNA silencing suppressor activity can still systemically infect pepper plants that carry *Tsw* and *N. benthamiana* plants (58, 59). Although these findings suggest that NSs protein is not absolutely required for virus systemic infection, the additional presence of viral RNA silencing suppressor NSs could significantly enhance replication and transcription of the S- and M-minireplicons lacking the NSs ORF in *N. benthamiana* cells. However, ectopic expression of NSs inhibited the rescue of the full-length $S_{(+)}$ segment from cDNA, indicating that the inhibition could be related to (simultaneous/a priori) ectopic expression of NSs gene sequences that overlap the full-length $S_{(+)}$ replicon. This possibility could be tested via ectopic expression of an untranslatable $NSs^{\Delta ATG}$ construct.

In summary, a series of issues has hampered the construction of a successful reverse genetics system for TSWV: the choice of promoter and construct design to generate primary viral RNA transcripts in plants that mimic authentic viral RNA molecules; the expression of a very large viral RdRp; negative effects of ectopic expression of RdRp, N, and NSs; and the absence of viral RNA synthesis of the wild-type $M_{(-)}$ segment. In the present

study, we were able to solve all these issues and established a reverse genetics system for TSWV with tripartite negative-stranded/ambisense RNA genomes. Using the S RNA minireplicon system containing eGFP and mCherry reporter genes, the role of *cis*- and *trans*-acting elements for viral replication and transcription can be studied. Using the M-RNA minireplicon system, cell-to-cell movement of TSWV RNPs in planta can be studied. To track the virus during systemic infection of plants, rTSWV can be generated containing fluorescent reporter genes at the genetic loci of either GP or NSs. The establishment of this RG system now provides us with a powerful platform to generate mutant viruses and study the basic principles of all aspects of viral infection cycle and their disease pathology in a natural setting.

Materials and Methods

Details of the methodology used are provided in *SI Appendix, Materials and Methods*, and include plasmid construction, plant material and growth conditions, agroinfiltration, immunoblot analysis, Northern blot analysis, RT-PCR, GFP imaging, fluorescence microscopy, and transmission electron microscopy. Primers used in this study are listed in *SI Appendix*, Table S3.

Data Availability. All data are available in the main text and *SI Appendix*.

ACKNOWLEDGMENTS. We thank Dr. Yi Xu for critical review of this manuscript. This work was supported by grants from the National Natural Science Foundation of China (Grants 31925032, 31630062, and 31870143), the Fundamental Research Funds for the Central Universities (Grant JCQY201904), the Youth Science and Technology Innovation Program (to X.T.), and the Postgraduate Research & Practice Innovation Program of Jiangsu Province (to M.F.).

1. M. K. David, M. H. Peter, *Fields Virology*, (Lippincott Williams & Wilkins, ed. 6, 2013), pp. 1–2264.
2. A. Plyusnin, R. M. Elliott, *The Bunyaviridae: Molecular and Cellular Biology* (Caister Academic Press, 2011), pp. 1–222.
3. T. L. German, D. E. Ullman, J. W. Moyer, Tospoviruses: Diagnosis, molecular biology, phylogeny, and vector relationships. *Annu. Rev. Phytopathol.* **30**, 315–348 (1992).
4. L. Kong, J. Wu, L. Lu, Y. Xu, X. Zhou, Interaction between Rice stripe virus disease-specific protein and host PsbP enhances virus symptoms. *Mol. Plant* **7**, 691–708 (2014).
5. G. Lu *et al.*, Tenuivirus utilizes its glycoprotein as a helper component to overcome insect midgut barriers for its circulative and propagative transmission. *PLoS Pathog.* **15**, e1007655 (2019).
6. J. E. Oliver, A. E. Whitfield, The genus tospovirus: Emerging bunyaviruses that threaten food security. *Annu. Rev. Virol.* **3**, 101–124 (2016).
7. M. Prins, R. Goldbach, The emerging problem of tospovirus infection and non-conventional methods of control. *Trends Microbiol.* **6**, 31–35 (1998).
8. M. Turina, R. Kormelink, R. O. Resende, Resistance to tospoviruses in vegetable crops: Epidemiological and molecular aspects. *Annu. Rev. Phytopathol.* **54**, 347–371 (2016).
9. A. E. Whitfield, D. E. Ullman, T. L. German, Tospovirus-thrips interactions. *Annu. Rev. Phytopathol.* **43**, 459–489 (2005).
10. M. Zhu, I. L. van Grinsven, R. Kormelink, X. Tao, Paving the way to tospovirus infection: Multilined interplays with plant innate immunity. *Annu. Rev. Phytopathol.* **57**, 41–62 (2019).
11. Q. Wang *et al.*, Rescue of a plant negative-strand RNA virus from cloned cDNA: Insights into enveloped plant virus movement and morphogenesis. *PLoS Pathog.* **11**, e1005223 (2015).
12. X. Yang *et al.*, Rice stripe mosaic virus, a novel Cytorhabdovirus infecting rice via leafhopper transmission. *Front. Microbiol.* **7**, 2140 (2017).
13. Q. Cao *et al.*, Transmission characteristics of Barley yellow striate mosaic virus in its planthopper vector Laodelphax striatellus. *Front. Microbiol.* **9**, 1419 (2018).
14. R. Kormelink, M. L. Garcia, M. Goodin, T. Sasaya, A. L. Haenni, Negative-strand RNA viruses: The plant-infecting counterparts. *Virus Res.* **162**, 184–202 (2011).
15. K. B. Scholthof *et al.*, Top 10 plant viruses in molecular plant pathology. *Mol. Plant Pathol.* **12**, 938–954 (2011).
16. M. J. Adams *et al.*, Changes to taxonomy and the international code of virus classification and nomenclature ratified by the international committee on taxonomy of viruses. *Arch. Virol.* **162**, 2505–2538 (2017).
17. H. R. Pappu, R. A. Jones, R. K. Jain, Global status of tospovirus epidemics in diverse cropping systems: Successes achieved and challenges ahead. *Virus Res.* **141**, 219–236 (2009).
18. S. A. Hogenhout, D. Ammar, A. E. Whitfield, M. G. Redinbaugh, Insect vector interactions with persistently transmitted viruses. *Annu. Rev. Phytopathol.* **46**, 327–359 (2008).
19. R. L. Gilbertson, O. Batuman, C. G. Webster, S. Adkins, Role of the insect supervectors Bemisia tabaci and Frankliniella occidentalis in the emergence and global spread of plant viruses. *Annu. Rev. Virol.* **2**, 67–93 (2015).
20. S. Adkins, R. Quadt, T. J. Choi, P. Ahlquist, T. German, An RNA-dependent RNA polymerase activity associated with virions of tomato spotted wilt virus, a plant- and insect-infecting bunyavirus. *Virology* **207**, 308–311 (1995).
21. P. de Haan *et al.*, Tomato spotted wilt virus L RNA encodes a putative RNA polymerase. *J. Gen. Virol.* **72**, 2207–2216 (1991).
22. Z. Feng *et al.*, The ER-membrane transport system is critical for intercellular trafficking of the NSm movement protein and tomato spotted wilt tospovirus. *PLoS Pathog.* **12**, e1005443 (2016).
23. R. Kormelink, M. Storms, J. Van Lent, D. Peters, R. Goldbach, Expression and subcellular location of the NSM protein of tomato spotted wilt virus (TSWV), a putative viral movement protein. *Virology* **200**, 56–65 (1994).
24. T. Soellick, J. F. Uhrig, G. L. Bucher, J. W. Kellmann, P. H. Schreier, The movement protein NSm of tomato spotted wilt tospovirus (TSWV): RNA binding, interaction with the TSWV N protein, and identification of interacting plant proteins. *Proc. Natl. Acad. Sci. U.S.A.* **97**, 2373–2378 (2000).
25. M. M. Storms, R. Kormelink, D. Peters, J. W. Van Lent, R. W. Goldbach, The nonstructural NSm protein of tomato spotted wilt virus induces tubular structures in plant and insect cells. *Virology* **214**, 485–493 (1995).
26. M. M. Storms *et al.*, A comparison of two methods of microinjection for assessing altered plasmodesmal gating in tissues expressing viral movement proteins. *Plant J.* **13**, 131–140 (1998).
27. M. Kikkert *et al.*, Tomato spotted wilt virus particle morphogenesis in plant cells. *J. Virol.* **73**, 2288–2297 (1999).
28. D. Ribeiro *et al.*, Tomato spotted wilt virus glycoproteins induce the formation of endoplasmic reticulum- and Golgi-derived pleomorphic membrane structures in plant cells. *J. Gen. Virol.* **89**, 1811–1818 (2008).
29. S. H. Sin, B. C. McNulty, G. G. Kennedy, J. W. Moyer, Viral genetic determinants for thrips transmission of Tomato spotted wilt virus. *Proc. Natl. Acad. Sci. U.S.A.* **102**, 5168–5173 (2005).
30. E. Bucher, T. Sijen, P. De Haan, R. Goldbach, M. Prins, Negative-strand tospoviruses and tenuiviruses carry a gene for a suppressor of gene silencing at analogous genomic positions. *J. Virol.* **77**, 1329–1336 (2003).
31. E. Schnettler *et al.*, Diverging affinity of tospovirus RNA silencing suppressor proteins, NSs, for various RNA duplex molecules. *J. Virol.* **84**, 11542–11554 (2010).
32. A. Takeda *et al.*, Identification of a novel RNA silencing suppressor, NSs protein of Tomato spotted wilt virus. *FEBS Lett.* **532**, 75–79 (2002).
33. N. H. Hoang, H. B. Yang, B. C. Kang, Identification and inheritance of a new source of resistance against tomato spotted wilt virus (TSWV) in Capsicum. *Sci. Hortic. (Amsterdam)* **161**, 8–14 (2013).
34. D. de Ronde *et al.*, Analysis of Tomato spotted wilt virus NSs protein indicates the importance of the N-terminal domain for avirulence and RNA silencing suppression. *Mol. Plant Pathol.* **15**, 185–195 (2014).
35. S. B. Kim *et al.*, Divergent evolution of multiple virus-resistance genes from a progenitor in Capsicum spp. *New Phytol.* **213**, 886–899 (2017).
36. J. Li *et al.*, Structure and function analysis of nucleocapsid protein of tomato spotted wilt virus interacting with RNA using homology modeling. *J. Biol. Chem.* **290**, 3950–3961 (2015).
37. K. Komoda, M. Narita, K. Yamashita, I. Tanaka, M. Yao, Asymmetric trimeric ring structure of the nucleocapsid protein of tospovirus. *J. Virol.* **91**, e01002–e01017 (2017).
38. Y. Guo *et al.*, Distinct mechanism for the formation of the ribonucleoprotein complex of tomato spotted wilt virus. *J. Virol.* **91**, e00892-17 (2017).
39. Z. Feng *et al.*, Nucleocapsid of Tomato spotted wilt tospovirus forms mobile particles that traffic on an actin/endoplasmic reticulum network driven by myosin XI-K. *New Phytol.* **200**, 1212–1224 (2013).
40. D. Ribeiro *et al.*, The cytosolic nucleoprotein of the plant-infecting bunyavirus tomato spotted wilt recruits endoplasmic reticulum-resident proteins to endoplasmic reticulum export sites. *Plant Cell* **25**, 3602–3614 (2013).
41. C. C. Brittlebank, Tomato diseases. *J Agric. Victoria* **27**, 231–235 (1919).
42. A. Bridgen, R. M. Elliott, Rescue of a segmented negative-strand RNA virus entirely from cloned complementary DNAs. *Proc. Natl. Acad. Sci. U.S.A.* **93**, 15400–15404 (1996).
43. G. Neumann *et al.*, Generation of influenza A viruses entirely from cloned cDNAs. *Proc. Natl. Acad. Sci. U.S.A.* **96**, 9345–9350 (1999).
44. L. Flatz, A. Bergthaler, J. C. de la Torre, D. D. Pinschewer, Recovery of an arenavirus entirely from RNA polymerase I/II-driven cDNA. *Proc. Natl. Acad. Sci. U.S.A.* **103**, 4663–4668 (2006).
45. U. Ganesan *et al.*, Construction of a Sonchus yellow net virus minireplicon: A step toward reverse genetic analysis of plant negative-strand RNA viruses. *J. Virol.* **87**, 10598–10611 (2013).
46. K. Ishibashi, E. Matsumoto-Yokoyama, M. Ishikawa, A tomato spotted wilt virus S RNA-based replicon system in yeast. *Sci. Rep.* **7**, 12647 (2017).
47. F. Ferron, F. Weber, J. C. de la Torre, J. Reguera, Transcription and replication mechanisms of Bunyaviridae and Arenaviridae L proteins. *Virus Res.* **234**, 118–134 (2017).
48. R. M. Elliott, Orthobunyaviruses: Recent genetic and structural insights. *Nat. Rev. Microbiol.* **12**, 673–685 (2014).
49. G. Blakqori, F. Weber, Efficient cDNA-based rescue of La Crosse bunyaviruses expressing or lacking the nonstructural protein NSs. *J. Virol.* **79**, 10420–10428 (2005).
50. T. Ikegami, S. Won, C. J. Peters, S. Makino, Rescue of infectious rift valley fever virus entirely from cDNA, analysis of virus lacking the NSs gene, and expression of a foreign gene. *J. Virol.* **80**, 2933–2940 (2006).

51. R. Flick, R. F. Pettersson, Reverse genetics system for Uukuniemi virus (Bunyaviridae): RNA polymerase I-catalyzed expression of chimeric viral RNAs. *J. Virol.* **75**, 1643–1655 (2001).
52. J. H. Doelling, R. J. Gaudino, C. S. Pikaard, Functional analysis of Arabidopsis thaliana rRNA gene and spacer promoters in vivo and by transient expression. *Proc. Natl. Acad. Sci. U.S.A.* **90**, 7528–7532 (1993).
53. J. Saez-Vasquez, C. S. Pikaard, Extensive purification of a putative RNA polymerase I holoenzyme from plants that accurately initiates rRNA gene transcription in vitro. *Proc. Natl. Acad. Sci. U.S.A.* **94**, 11869–11874 (1997).
54. A. Martin, P. Staeheli, U. Schneider, RNA polymerase II-controlled expression of antigenomic RNA enhances the rescue efficacies of two different members of the Mononegavirales independently of the site of viral genome replication. *J. Virol.* **80**, 5708–5715 (2006).
55. É. Bergeron *et al*., Reverse genetics recovery of Lujo virus and role of virus RNA secondary structures in efficient virus growth. *J. Virol.* **86**, 10759–10765 (2012).
56. A. Pekosz, B. He, R. A. Lamb, Reverse genetics of negative-strand RNA viruses: Closing the circle. *Proc. Natl. Acad. Sci. U.S.A.* **96**, 8804–8806 (1999).
57. R. Flick, K. Flick, H. Feldmann, F. Elgh, Reverse genetics for crimean-congo hemorrhagic fever virus. *J. Virol.* **77**, 5997–6006 (2003).
58. P. Margaria, M. Ciuffo, D. Pacifico, M. Turina, Evidence that the nonstructural protein of Tomato spotted wilt virus is the avirulence determinant in the interaction with resistant pepper carrying the TSW gene. *Mol. Plant Microbe Interact.* **20**, 547–558 (2007).
59. P. Margaria *et al*., The NSs protein of tomato spotted wilt virus is required for persistent infection and transmission by Frankliniella occidentalis. *J. Virol.* **88**, 5788–5802 (2014).